UNIVERSITAT POLITÈCNICA
DE CATALUNYA

Robust Exact Differentiation via Sliding Mode Technique applied to a Fixed-Frequency Quasi-Sliding Control Algorithm

D. Biel, E. Fossas, C. Meza, R. Muñoz.

ACES – Control avançat de sistemes d'energia

IOC-DT-P-2008-01
Gener 2008

Institut d'Organització i Control
de Sistemes Industrials

Robust Exact Differentiation via Sliding Mode Technique applied to a Fixed-Frequency Quasi-Sliding Control Algorithm.

D. Biel, E. Fossas, C. Meza, R. Muñoz
Institute of Industrial and Control Engineering
Technical University of Catalonia

January, 2008

Abstract

This paper presents the design of a DC-AC power converter controller that bears the same benefits of a sliding mode controller but with the advantage of a fixed-frequency control signal. The controller is based on the imposition of zero averaged value of the sliding surface in each switching cycle. A keypoint of the presented controller is the calculation of the sliding surface's derivative which in the present paper is obtained using an estimation algorithm introduced by Levant in 1998.

1 Introduction

A switching power converter can be modeled as a variable structure system due to the different topologies that the circuit, controlled by a discontinuous control action, can achieve. This kind of systems (variable structure bilinear systems) are well suited to be controlled by means of a sliding mode controller.

The published work by [15], [13] and, [5] where among the first published work in which switching power converters were controlled using a sliding mode controller. The first two papers deal with DC-DC conversion while the third one focuses on DC-AC conversion. The control laws proposed in those articles meet the initial specifications and the robustness against load and line variations.

Sliding mode controllers were initially implemented using zero-order holders or hysteresis comparators. The major drawback with this kind of implementation is that the closed-loop system will present a variable switching frequency and harmonics due to the spreading of the switching along all the band of frequencies. Therefore, due to this asynchronous switching, the controlled system will present a wideband frequency spectrum that difficults the design of the output filter and may present some distrubances caused by this unmodeled dynamics. On the other hand, an implementation by means of a pulse-width modulator (PWM) guaranties a fixed switching frequency. In this case the

switching harmonics are located in multiples of the switching frequency (usually greater or equal than 10 kH) which simplifies significantly the design of the output filter. Besides, given that in general the dynamic system modulus is discontinuous over the sliding surface, the implementation by means of a PWM results in a better performance compared to the zero-order hold implementations.

The problem of the implementation of sliding mode controllers has gathered the attention of diverse authors. For example [3], [4] and [9] propose to add an hysteresis cycle to the sliding mode control comparator. In [11] and [8] a sliding mode implementation with a variable band hysteresis cycle is also mentioned. Other implementations, like the ones reported in [12] and [10], propose a sliding mode controller with a pulse width modulator in which the switching frequency is synchronized by means of an external signal. In [14] the PWM's duty ration is directly computed from the equivalent control.

The "Zero Average Dynamics" (ZAD) control scheme proposed in [6], offers the advantages of a fixed-frequency implementation and the inherent robustness of a sliding mode controller. This scheme is based in:

- the adequate design of the sliding surface to accomplish all the specifications and
- the specific calculation of the PWM's duty ration in order to obtain a null averaged value of the sliding surface calculated in one switching period.

In [2] a survey of the different electronic implementations of sliding mode controller in power converters is presented. It also includes a comparative analysis of the ZAD algorithm with respect to the other implementations.

The specifications of DC-AC conversion requires a zero error in the AC tracking output signals and robustness with the respect to load and line variations. In some applications the load is highly variable like in the cases in which an inverter is connected to a passive rectifier or when diverse sodium lamps are suddenly connected to the inverter. The latter is equivalent to a highly variable output capacitance.

There are different ways in which a PWM can be implemented. The most widely used ones consist on a comparison between the reference signal and a sawtooth or a triangular carrier waveform. The carrier waveform determines which edge of the resultant pulse is modulated; based on this, PWM implementations are usually classified as: leading edge modulation (increasing sawtooth carrier), trailing edge modulation (decreasing sawtooth carrier) and centered pulses in which both edges are modulated (triangular carrier).

In the present work a fixed-frequency quasi-sliding control algorithm is presented and implemented by means of a pulse-width modulator. The algorithm, based on the ZAD strategy for the signal tracking in DC-AC inverters, directly generates the PWM's duty ratio. Two requirements are needed in order to obtain a correct behavior of the proposed algorithm: to obtain a linear piece-wise sliding surface and to achieve a good estimation of the sliding surface's slopes. In general, the power converters satisfies the first requirement due to the fact that the inductor's current represents the dominant term of the sliding surfaces; the inductor's current has an approximate linear piece-wise behavior. With respect to the second requirement, different approximations of the sliding surface's slopes are considered based on the number of the samples taken in one switching period. Special attention is given to a slope approximation based on the exact differentiator introduced by Levant in 1998.

The present paper is organized in the following way: in section 2 a summary of the ZAD control is presented. Section 4 deals with the complete modeling of the power converter

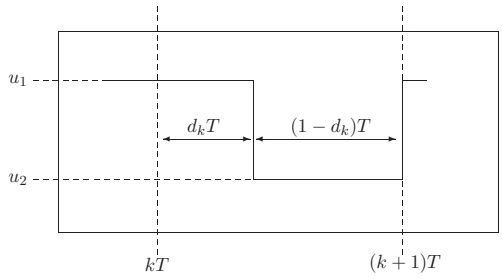

Figure 1: Examples of Pulse Width Modulation.

and the control algorithm. Given its relevance in the control algorithm the sliding surface's slope estimation is presented in a specific section (section 3). The proposed algorithm is validated and its different implementations are compared with the simulation results presented in section 5. The conclusions end the article in section 6.

2 ZAD control scheme.

In this section the ZAD control scheme set out in [6] is revisited.

Let be a SISO, autonomous system

$$\dot{\mathbf{x}} = f(\mathbf{x}) + g(\mathbf{x})u \tag{1}$$

where $\mathbf{x} \in \mathbb{R}^n$, $u \in \mathbb{R}$ and f and g are smooth vector fields. Let us assume it is governed by a switching surface

$$\Sigma = \{(\mathbf{x}, t) \,|\, \sigma(\mathbf{x}, t) = 0\} \tag{2}$$

and a control law

$$u = \begin{cases} u^+ & \text{if } \sigma(\mathbf{x}, t) > 0 \\ u^- & \text{if } \sigma(\mathbf{x}, t) < 0 \end{cases} \tag{3}$$

so that there are sliding modes on Σ.

Let us assume too that this control action is implemented using a Pulse Width Modulator (PWM) (Fig. 1)

$$u_{PWM} = \begin{cases} u_1 & t \in [kT, (d_k)\,T) \\ u_2 & t \in [(d_k)\,T, (k+1)\,T) \end{cases} \tag{4}$$

where T is the switching period, d_k is the duty cycle in period k and $u_1 = \max\{u^+, u^-\}$ (resp. $u_2 = \min\{u^+, u^-\}$).

As it was already reported in [14], sliding control modes can be implemented using pulse width modulators. Then, the relationship between the duty cycle and the equivalent control is given by

$$d_k = \frac{u_{eq} - u_2}{u_1 - u_2} \tag{5}$$

provided that $u_2 \leq u_{eq} \leq u_1$. However, the equivalent control may depend on system parameters, hence a nominal duty cycle can be computed in this way only, and the

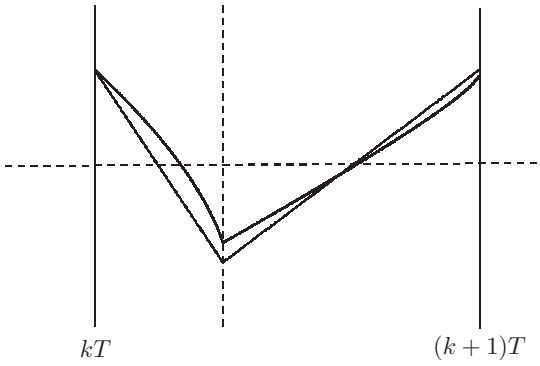

Figure 2: Sliding surface and its piecewise linear approximation.

robustness common in Sliding Control Modes may be wasted. Instead, a new strategy was proposed in [6]. Namely, a duty cycle direct design so that the average of the sliding surface on each switching period is zero. Some theoretical results on this approach particularised to second order linear systems can be found in [1].

Let us assume that the sliding surface can be approximated by a piece-wise linear function as in (Fig. 2) then, the ZAD duty-cycle d_k is given by

$$\hat{d}_k = 1 - \sqrt{\frac{\left|\frac{d\sigma_k}{dt}\,|_{u=u_1}\right| - \frac{2\sigma_k}{T}}{\left|\frac{d\sigma_k}{dt}\,|_{u=u_1}\right| + \left|\frac{d\sigma_k}{dt}\,|_{u=u_2}\right|}} \quad \text{if } \sigma_k > 0 \tag{6}$$

$$\hat{d}_k = 1 - \sqrt{\frac{\left|\frac{d\sigma_k}{dt}\,|_{u=u_2}\right| + \frac{2\sigma_k}{T}}{\left|\frac{d\sigma_k}{dt}\,|_{u=u_1}\right| + \left|\frac{d\sigma_k}{dt}\,|_{u=u_2}\right|}} \quad \text{if } \sigma_k < 0 \tag{7}$$

and

$$d_k = \mathtt{sat}\left(\hat{d}_k\right) \tag{8}$$

presuming the radicand is positive; otherwise the signal saturates. The pulse starts with $u = u_1$ ("trailing") if $\sigma_k > 0$ and with $u = u_2$ ("leading") if $\sigma_k < 0$.

Subindex k means that functions are evaluated at $t = kT$ and $\mathtt{sat}\left(\hat{d}_k\right) \in [0, 1]$.

3 The Levant Exact Differentiator.

In the actual system, sampling and data processing takes some time. Thus,

$$\sigma_k, \quad \dot{\sigma}_{k_{|u=u_1}} \text{ and } \dot{\sigma}_{k_{|u=u_2}}$$

must be estimated during the time period $[(k-1)T, kT)$. The Robust Exact Differentiator via Sliding Mode Technique [7] is used to estimate $\dot{\sigma}_{k_{|u=u_1}}$ and $\dot{\sigma}_{k_{|u=u_2}}$. The main results appeared in [7] are stated below:

In order to differentiate the unknown signal f, the modified second order sliding algorithm can be considered as follows

$$\left\{\begin{array}{rcl} \dot{x} & = & u \\ u & = & u_1 - \lambda|x - f(t)|^{\frac{1}{2}}\mathtt{sign}(x - f(t)) \\ u_1 & = & -\alpha\mathtt{sign}(x - f(t)) \end{array}\right. \tag{9}$$

where α, $\lambda > 0$. *Here* $u(t)$ *is the output of the differentiator.*

Define the function $\phi(\alpha, \lambda, C) = |\Psi(t_*)|$ *where* (Σ, Ψ) *is the solution of*

$$\begin{array}{rcl} \dot{\Sigma} & = & -|\Sigma|^{\frac{1}{2}} + \Psi \\ \dot{\Psi} & = & \left\{\begin{array}{ll} -\frac{1}{\lambda^2}(\alpha - C) & \text{if } -|\Sigma|^{\frac{1}{2}} + \Psi > 0 \\ -\frac{1}{\lambda^2}(\alpha + C) & \text{if } -|\Sigma|^{\frac{1}{2}} + \Psi \leq 0 \end{array}\right. \end{array}$$

$\Sigma(0) = 0$, $\Psi(0) = 1$, $t_* = \inf\{t \,|\, t > 0$ *and* $\Sigma(t) = 0$ *and* $\Psi(t) < 0\}$. *Now the theorem*

Let $\alpha > C > 0$, $\lambda > 0$, $\phi(\alpha, \lambda, C) < 1$. *Then,* $u(t) = \dot{f}(t)$ *fulfils identically after a finite time provided that* $\dot{f}$ *has a Lipschitz constant* C. *The less* $\psi(\alpha, \lambda, C)$, *the faster the convergence.*

Levant algorithm is applied to get $\dot{\sigma}$ which is a piecewise continuous function. Its derivative is discontinuous at switching instants. However

$$\dot{\sigma}_{u=u_1} - \dot{\sigma}_{u=u_2} = \left(\frac{\partial \sigma}{\partial \mathbf{x}} g\right)(u_1 - u_2). \tag{10}$$

Thus, if the right hand side of equation 10 is independent of the plant parameters and computable from measured variables, as particularly happens in power converters, the estimation of one of the derivatives is enough for knowing the other one. Hence, using Levant algorithm on $\sigma(\mathbf{x}(t), t)$, both $\dot{\sigma}_{u=u_1}$ and $\dot{\sigma}_{u=u_2}$ are obtained[1], the former directly from the algorithm in the first and third subperiods, while the latter using equation 10. On the other way around, in the second subperiod, $\dot{\sigma}_{u=u_2}$ is directly estimated while $\dot{\sigma}_{u=u_1}$ is computed using the equation.

Actually, equation 10 is used at switching instants. Namely, let us assume there is a commutation at $t = t^*$. There is no loss of generality to assume that the switch commutes from u_1 to u_2. Hence, $\dot{\sigma}_{\mathbf{x}(t^*),u=u_1}$ is known and using equation 10 $\dot{\sigma}_{\mathbf{x}(t^*),u=u_2}$ is known as well. The latter will be used as initial conditions in equation 9 for the second subperiod. In this way, it would not be any transient due to the initial conditions when estimating the derivative in a new subperiod and Levant algorithm is in steady-state always.

4 The Whole Model.

In this section the ZAD-PWM algorithm is applied to the full-bridge high-frequency inverter depicted in (Fig. 3). The model of the plant is described in subsection 4 as well as the continuous time sliding mode control algorithm. The derivatives of the switching surface are estimated in subsection 4.2 while, in subsection 4.3 a digital implementation procedure is described.

[1]Remark that these derivatives can not be obtained from the dynamical system because we are interested in a robust control system.

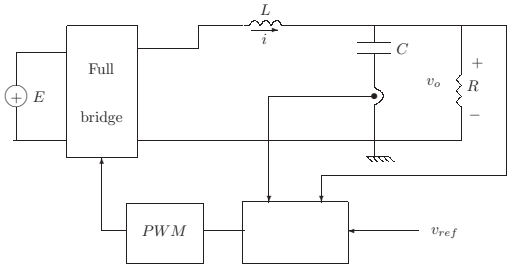

Figure 3: Full bridge high-frequency inverter.

4.1 The buck converter.

The power inverter is modelled by

$$L\frac{di_L}{dt} = Eu - v_o \tag{11}$$

$$C\frac{dv_o}{dt} = i - i_l \tag{12}$$

where i is the inductor current, v_o is the output voltage, i_l is the load current, which takes different waveforms depending on the load, L is the inductance, C is the capacitor and E is the input voltage. The control signal u drives the power switches states (IGBT's in this case) and takes discrete values; namely, $u \in \{-1, 1\}$, this resulting in an LC filter input voltage of $-E$ or $+E$. The desired AC regulated output voltage is achieved by designing a sliding control loop based on the following switching surface proposed by Carpita et al. in [5]

$$\hat{\sigma}(\mathbf{x}, t) \triangleq (V_{ref}(t) - v_o(t)) + \hat{\tau}\left(\frac{V_{ref}(t) - v_o(t)}{dt}\right) \tag{13}$$

and the control law

$$u = \begin{cases} +1 & \text{if } \hat{\sigma}(\mathbf{x}(t), t) > 0 \\ -1 & \text{if } \hat{\sigma}(\mathbf{x}(t), t) < 0 \end{cases} \tag{14}$$

where $V_{ref}(t) = A\sin(2\pi f t)$ is the reference signal and τ is a user-defined parameter. This design leads to the desired steady state sliding motion, that is, $v_o(t) = V_{ref}(t) = A\sin(2\pi\ f\ t)$.

For simplicity this model will be written in normal form using dimensionless variables and parameters. Let us take the change of variables

$$t = \sqrt{LC}r, \quad z_1 = \frac{v_0}{E}, \quad z_2 = \frac{dz_1}{dr}$$

then, the whole dynamics results in

$$\frac{dz_1}{dr} = z_2 \tag{15}$$

$$\frac{dz_2}{dr} = u - z_1 - l \tag{16}$$

$$\sigma(\mathbf{x}, r) = z_{1d} - z_1 + \tau(z_{2d} - z_2) \tag{17}$$

$$u = \begin{cases} +1 & \text{if } \sigma(\mathbf{x}(r), r) > 0 \\ -1 & \text{if } \sigma(\mathbf{x}(r), r) < 0 \end{cases} \tag{18}$$

where $z_{1d} = \frac{V_{ref}}{E}$, $z_{2d} = \frac{dz_{1d}}{dr}$, $l = \frac{L}{E}\frac{di_l}{dt}$ and $\tau = \sqrt{LC}\hat{\tau}$.

Particularising equation 10 to this case results in

$$\dot{\sigma}_{u=u_1} - \dot{\sigma}_{u=u_2} = 2\tau. \tag{19}$$

Hence, as it is mentioned in section 3, the estimation of one of the derivatives of σ ($u = u_1$ or $u = u_2$) is enough for to know both of them ($u = u_1$ and $u = u_2$).

4.2 Estimating derivatives.

There is no loss of generality in assuming that $\dot{\sigma}_{|u=u_1}$ is the derivative to be estimated. Note that a Lipschitz constant C of $\dot{\sigma}_{|u=u_1}$ is needed in order to apply Levant algorithm. To this end $\ddot{\sigma}_{|u=u_1}$ will be considered. Actually, we are looking for a bound for it. Then, the mean value theorem allows us to use this bound as Lipschitz constant for $\ddot{\sigma}_{|u=u_1}$.

For simplicity let us assume $l = \gamma z_2$, this is not a constrain really; the general result can be obtained using similar arguments.

Solving the linear dynamics for $u = u_1$ yields

$$\begin{aligned}\sigma_{|u=u_1}(\mathbf{x}(r), r) &= A\sin(2\pi f r) - \left(e^{\frac{-r\gamma}{2}} f_1(r, u_1) + u_1\right) + \\ &\quad \tau\left(2A\pi f\cos(2\pi f r) - \left(e^{\frac{-r\gamma}{2}} f_2(r, u_2)\right)\right)\end{aligned}$$

where $f_1(r, u_1)$ and $f_2(r, u_1)$ are bounded. The second derivative results in

$$\begin{aligned}\ddot{\sigma}_{|u=u_1}(\mathbf{x}(r), r) &= 4A\pi^2 f^2\sin(2\pi f r) - \left(e^{\frac{-r\gamma}{2}} h_1(r, u_1)\right) + \\ &\quad \tau\left(8A\pi^3 f^3\cos(2\pi f r) - \left(e^{\frac{-r\gamma}{2}} h_2(r, u_1)\right)\right)\end{aligned}$$

for some bounded functions $h_1(r, u_1)$, $h_2(r, u_2)$. Since the Lipschitz constant is needed when the ZAD algorithm does not saturate, $\sigma_{|u=u_1}$ and $\ddot{\sigma}_{|u=u_1}$ as well can be presumed in steady-state. Thus, the latter can be approximated by

$$\ddot{\sigma}_{|u=u_1}(\mathbf{x}(r), r) \simeq 4A\pi^2 f^2\sin(2\pi f r) + \tau 8A\pi^3 f^3\cos(2\pi f r) \tag{20}$$

and, finally

$$\left|\ddot{\sigma}_{|u=u_1}\right| \leq 4A\pi^2 f^2\sqrt{1 + 4\tau^2\pi^2 f^2} \triangleq \hat{C} \tag{21}$$

Hence, by the mean value theorem

$$\left|\dot{\sigma}_{|u=u_1}(\mathbf{x}(r_1), r_1) - \dot{\sigma}_{|u=u_1}(\mathbf{x}(r_2), r_2)\right| \leq \hat{C}|r_1 - r_2| \tag{22}$$

The same Lipschitz constant C was obtained if $u = u_2$ instead of $u = u_1$ in equation 20 because both $u = u_1$ and $u = u_2$ are constant.

4.3 The ZAD PWM digital algorithm.

Based on the reported results, a fixed frequency digital control scheme is implemented (Fig. 4). Although the PWM frequency is 20kH, the switching surface is sampled at

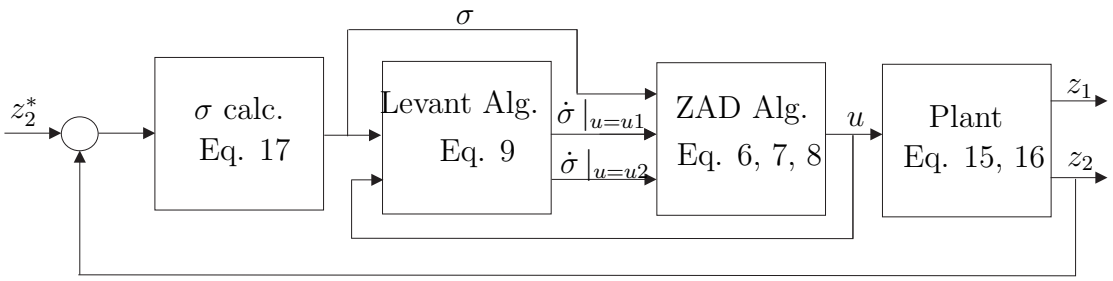

Figure 4: Quasi-sliding control algorithm

$E = 70V$	$v_0 = 45\sin(100\pi t)$	$L = 2mH$
$C = 40\mu F$	$k = 1000$	$T_m = 0.5\mu s$
$R_{Load} = 5\Omega$	$\alpha \approx 5.35 * 10^9$	$\lambda \approx 1.81 * 10^7$

Table 1: Simulation data

a frequency of 400kH to appropriately estimate the switching surface derivative. As in Levant's paper [7], parameters α and λ fulfill

$$\alpha > C \tag{23}$$

$$\lambda^2 \geq 4C\frac{\alpha + C}{\alpha - C} \tag{24}$$

where C is the Lipschitz constant defined in Equation (21). Then, the sliding surfaces derivatives are calculated taking into account the correction in the initial condition at switching times.

5 Simulation Results.

System response using an ideal differentiator and the Levant approximation is depicted in (Fig. 5) and (Fig.6). Plant parameters are in Table 1. The output voltage and the reference are compared in (Fig. 5(a)) and (Fig. 6(a)) while the errors are depicted in (Fig. 5(b)) and (Fig. 6(b)). The sliding surface and its derivative obtained through the Levant differentiator are shown in (Fig. 5(c)) and (Fig. 6(c)) and in (Fig. 5(d)) and (Fig. 6(d)) respectively. Note that the results are really close this meaning that the use of the Levant differentiator is appropriate.

The system answer to load changes is depicted in (Fig. 7). System starts with nominal values, then the circuit is open for $t \in [0.005, 0.025]$ and the load is connected again at $t = 0.025$. Note that the new algorithm is robust in front of load changes.

6 Conclusions.

The Levant robust exact differentiator has proved to be very useful for solving a keypoint in a quasi-sliding control algorithm, namely the estimation of the sliding (switching)

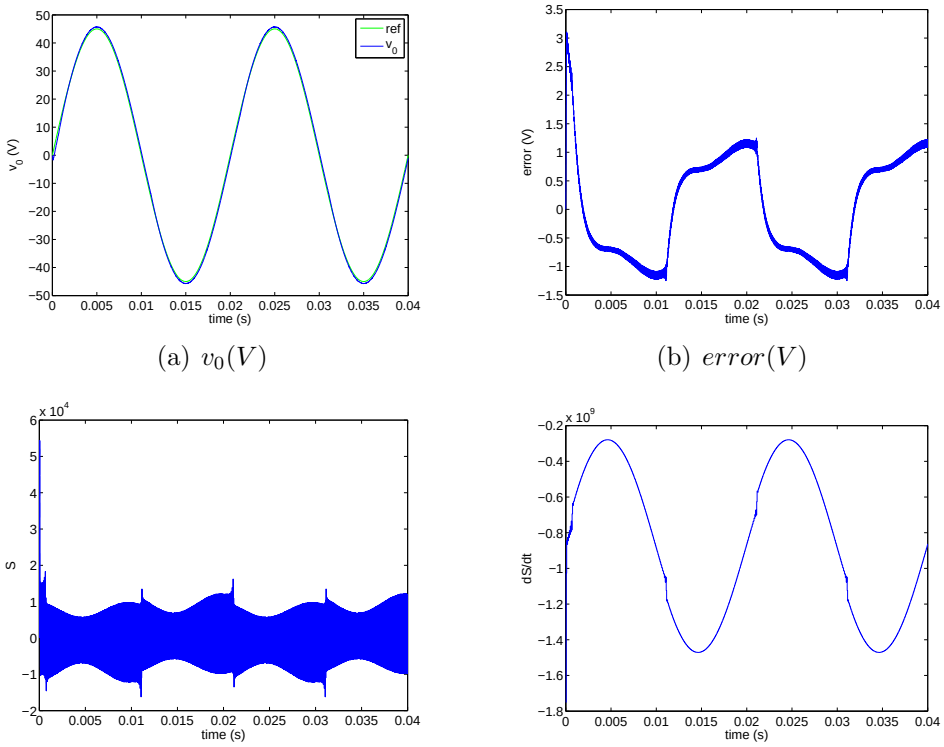

(a) $v_0(V)$ (b) $error(V)$

(c) S (d) $\dot{S}$

Figure 5: System response computing exact derivatives

surface derivatives. The improved control scheme has been applied to get a DC/AC inverter robust with respect to load perturbations.

References

[1] F. Angulo, E. Fossas, and T.M. Seara. Applied perturbation theory to power converters regulation. In *Proceedings of ENOC-2005*, Eindhoven, The Netherlands, August, 7-12 2005.

[2] D. Biel and E. Fossas. Smc applications in power electronic conversion. In A. Sabanovic, L. Fridman, and S. Spurgeon, editors, *Variable Structure Systems: from principles to implementation*, pages 265 – 293. Institution of Electrical Engineers (IEE), 2004.

[3] F. Bilalović, O. Mušić, and A. Šabanović. Buck converter regulator operating in the sliding mode. *Proceedings VII International PCI*, pages 331–340, 1983.

[4] H. Bühler. *Réglage par mode de glissement*. Presses Polytechniques Romandes, 1986.

[5] M. Carpita, M. Marchesioni, M. Oberti, and L. Puguisi. Power conditioning system using sliding mode control. In *Proceedings of the 19th Annual IEEE Power Electronics Specialist Conference*, pages 623 – 633, Kyoto, Japan, April, 11-14 1988.

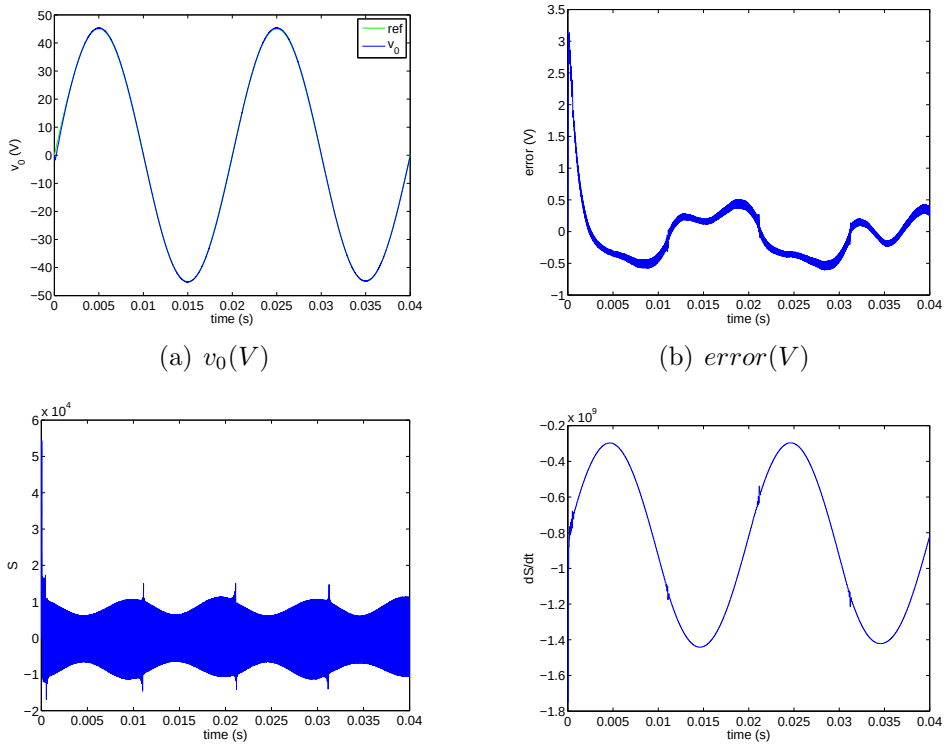

(a) $v_0(V)$ (b) $error(V)$

(c) S (d) $\dot{S}$

Figure 6: System response using the Levant differentiator

[6] E. Fossas, R. Griñó, and D. Biel. Quasi-sliding control based on pulse width modulation, zero averaged dynamics and the l2 norm. In Xinghuo Yu and Jian-Xin Xu, editors, *Advances in Variable Structure Systems, analysis, integration and applications*, pages 335 – 344. World Scientific, Singapore, 2001.

[7] A. Levant. Robust exact differentiation via sliding mode technique. *Automatica*, 34(3):379 – 384, March 1998.

[8] L. Malesani, L. Rossetto, G. Spiazzi, and A. Zuccato. An ac power supply with sliding-mode control. *IEEE Industry Applications Magazine*, pages 32–38, 1996.

[9] B. Nicolas, M. Fadel, and Y. Chéron. Sliding mode control of dc-to-dc converters with input filter based on the lyapunov-function approach. *Proceedings of European Power Electronics Conference (EPE)*, pages 1338–1343, 1995.

[10] H. Pinheiro, A.S. Martins, and J.R. Pinheiro. A sliding mode controller in single phase voltage source inverters. *International Conference on Industrial Electronics Control and Instrumentation (IECON)*, pages 394–398, 1994.

[11] J.M. Ruiz, S. Lorenzo, I. Lobo, and J. Amigo. Minimal ups structure with sliding mode control and adaptive hysteresis band. *Proceedings of International Conference on Industrial Electronics Control and Instrumentation (IECON)*, pages 1063–1067, 1990.

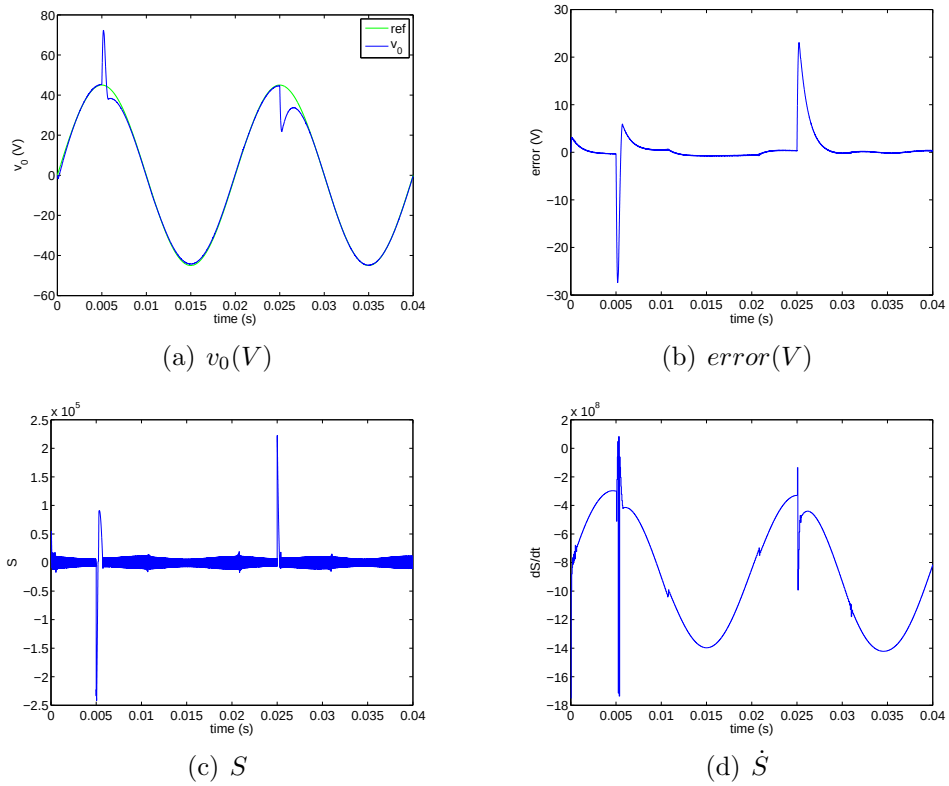

(a) $v_0(V)$ (b) $error(V)$

(c) S (d) $\dot{S}$

Figure 7: System response at load change using the Levant differentiator

[12] J.F. Silva and S.S. Paulo. Fixed frequency sliding modulator for current mode pwm inverters. *Proceedings of Power Electronic Specialist Conference (PESC)*, pages 623–629, 1993.

[13] H. Sira-Ramírez. Sliding motions in bilinear switched networks. *IEEE Transactions on Circuits and Systems*, 34(8):919 – 933, August 1987.

[14] H. Sira-Ramírez. A geometric approach to pulse-width modulated control in nonlinear dynamical systems. *IEEE Transactions on Automatic Control*, 34(2):184 – 187, Febrero 1989.

[15] R. Venkataramanan, A. Sabanovic, and S. Cuk. Sliding mode control of dc-to-dc converters. In *Proceedings of the 1985 Conference of the IEEE Industrial Electronics Society*, pages 251 – 258. MIT Press, 1985.